Flow past 6:1 prolate spheroid - A numerical study

A. Rajesh * K. N. Vinay Kumar † M. B. Subrahmanya‡ D. S. Kulkarni‡ B.N.Rajani ‡

* *Project Assistant, CTFD Division, CSIR-NAL, Bangalore 560 017, India*

†*Student, Dept. of Mech. Engg, SSIT Tumkur 572 107, India*

‡*Scientist, CTFD Division, CSIR-NAL, Bangalore 560 017, India*

Abstract

Numerical simulation of the three dimensional flow past $6:1$ prolate spheroid at $\alpha = 20^\circ$ and $Re = 4.2 \times 10^6$ using RANS approach has been carried out using the parallel version of the in-house structured grid multiblock flow solution code 3D-PURLES. The SST turbulence model is used to simulate the fully turbulent case and this model is suitably modified to handle transitional flows by fixing the onset of transition. The results thus obtained are validated against the available measurement and/or computational data.

Keywords: Prolate spheroid, SST turbulence model, fixed transition, finite volume method, parallel computing.

1 Introduction

Three dimensional flow past prolate spheroids with different aspect ratios can be considered as simplified models of submarines, unmanned underwater vehicles, missiles, airships *etc*. The prolate spheroids are geometrically simple but the flow characteristics are dominated by complex flow phenomenon like separation and transition. The three dimensional transitional flow with separation is one of the most challenging problems in fluid dynamics. Inspite of continuous research, the physics of three dimensional separation and the process of transition is not yet fully understood. The lack of proper understanding and non-availability of appropriate and accurate models for separated turbulent and transitional flows forms a stumbling block for accurate flow predictions using the CFD tools. Several measurements and simulations for flow over prolate spheroids have been documented for surface pressure and skin friction coefficient, profile of mean and turbulence quantities and also details of the separated region at various angle of attack [1, 4]. The paper presents the flow around $6:1$ prolate spheroid at 20° angle of attack for $Re = 4.2 \times 10^6$ for which experimental data [2, 12] and LES computation results [4] are available. The present simulation has been carried out using the in-house flow solution code 3D-PURLES treating the flow to be fully turbulent and also by fixing the onset of transition based on measurement data.

2 Finite Volume Method

2.1 Governing Equations

The phase-averaged Navier Stokes equation for unsteady turbulent incompressible flow in *non-orthogonal curvilinear coordinates* with cartesian velocities as dependent variables in a compact form are as follows:

Momentum transport for the Cartesian velocity component $\langle U_i \rangle$:

$$\frac{\partial}{\partial t}\left(\rho\langle U_i\rangle\right) + \frac{1}{J}\frac{\partial}{\partial x_j}\left[\rho\langle U_i\rangle\langle U_k\rangle\beta_k^j + \langle P\rangle\beta_i^j - \frac{\mu}{J}\left(\frac{\partial\langle U_i\rangle}{\partial x_m}B_m^j + \frac{\partial\langle U_k\rangle}{\partial x_m}\beta_i^m\beta_k^j\right) - \rho\langle u_i u_j\rangle\beta_k^j\right] = S_{U_i} \qquad (1)$$

*Corresponding author. Email: rajeshamech@gmail.com

where, $\langle P \rangle$ and $\langle U_i \rangle$ are the phase-averaged pressure and velocity components along i direction respectively. μ is the fluid viscosity, B_k^j and b_k^j are the metric coefficients due to transformation from cartesian to curvilinear coordinates and J is the Jacobian of the transformation matrix. u_i is the fluctuating velocity components and S_{U_i} is any momentum source other than the pressure gradient These momentum equations are further supplemented by the mass conservation or the so-called continuity equation.

Mass conservation (Continuity):

$$\frac{\partial}{\partial x_j}\left(\rho\langle U_k\rangle\beta_k^j\right) = 0 \tag{2}$$

The unknown turbulent stress term $-\rho\langle u_i u_j\rangle$ is defined as follows based on the eddy viscosity hypothesis

$$-\rho\langle u_i u_j\rangle = \mu_t\left(\frac{\partial\langle U_i\rangle}{\partial x_j} + \frac{\partial\langle U_j\rangle}{\partial x_i}\right) - \frac{1}{3}\rho\delta_{ij}\langle u_k u_k\rangle \tag{3}$$

where, δ_{ij} is the Kronecker Delta and μ_t is the eddy viscosity which is an isotropic scalar quantity. The eddy viscosity is evaluated through turbulence modelling.

2.2 Numerical Solution of Finite Volume Equation

The present computation uses a general geometry, multiblock structured, pressure-based implicit finite volume algorithm 3D-PURLES, developed at the CTFD Division, NAL Bangalore to solve the unsteady turbulent incompressible flow [8]. Central difference and other higher order upwind schemes have been used for spatial discretisation of the convective fluxes whereas the temporal derivatives are discretised using the second order accurate three-level fully implicit scheme. An iterative decoupled approach similar to the SIMPLE algorithm [7], modified for collocated variable arrangement [5] is adopted to avoid the checkerboard oscillations of the flow variables. The system of linear equations derived from the finite volume procedure is solved sequentially for the velocity components, pressure correction and turbulence scalars using the strongly implicit procedure of Stone [10]. The algorithm is also successfully parallelized for cost effective computation on multiple processors using standard MPI routines. The present parallel computations have been carried out on the Altix-Ice cluster.

3 Results and Discussion

In this study two different grids with O-O topology have been used (i) Coarse grid- $111 \times 101 \times 312$ covered by 24 blocks and (ii) Fine grid- $251 \times 161 \times 624$ covered by 48 blocks. The non-dimensionalised near wall distance for both the grids are maintained to be less than one. The schematic representation of the boundary condition and grid used are shown in Fig. 1. The unsteady computations have been carried out for $Re = 4.2 \times 10^6$ based on the model length (L) at $\alpha = 20^\circ$ using the central difference scheme (CDS) coupled to deferred correction procedure [3] for spatial discretisation of convective flux and a second order accurate scheme for temporal discretisation with the non-dimensionalised time step size of $\Delta t = 0.05$. The simulations have been carried out assuming the flow to be fully turbulent and also by fixing the transition onset location. The Shear Stress Transport (SST) model proposed by Menter [6] and the one equation model of Spalart-Allamaras (SA) [9] have been used for the fully turbulent case. In the fixed transition case, the flow is tripped by fixing the transition onset location. The flow is treated as laminar $(\mu_t = 0)$ upto the trip location and in the downstream μ_t is computed using the specified turbulence model which is SST model in the present computation. Uniform flow is assumed at the farfield boundary with freestream turbulence maintained at one percent and assuming the local eddy viscosity (μ_t) to be equal to the laminar viscosity (μ).

The effect of grid resolution on the azimuthal variation of the surface pressure coefficient (C_p) at two different axial locations $(X/L = 0.44$ and $0.77)$ obtained using SST turbulence model for $\alpha = 20^\circ$ is shown in Fig. 2. The figure clearly indicates that refining the grid brings no significant change in the variation of the pressure coefficient

which is also reflected in the aerodynamic coefficient (Table. 1). The effect of turbulence model for the coarse grid resolution on the azimuthal variation of the surface pressure coefficient at the two axial locations for $\alpha = 20^{\circ}$ is shown in Fig. 3. The figure clearly indicate that the SST turbulence model is in better agreement with the measurement data [2]. The deviation observed in the results obtained by SA model needs further investigation.

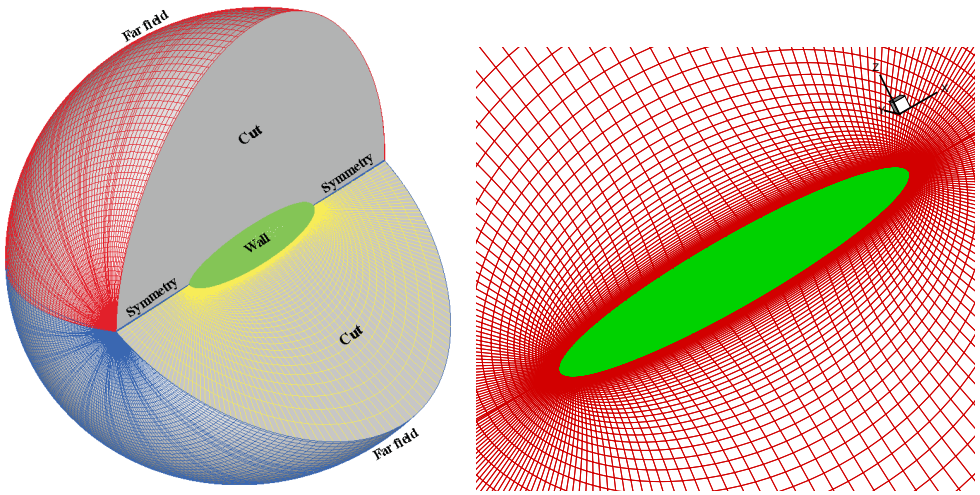

(a) Boundary conditions (b) Near wall view of surface grid

Figure 1: Boundary condition and multiblock grid used for flow past prolate spheroid

Grid resolution	C_l	C_d	C_m
Coarse - $111 \times 101 \times 312$	0.0366	0.0176	-0.0206
Fine - $251 \times 161 \times 624$	0.0371	0.0170	-0.0210

Table 1: Effect of grid size on aerodynamic coefficients

Simulations have also been carried out by fixing the transition onset location at $X/L = 0.2$ based on the measurement data [2, 11]. in the SST turbulence model. The surface streamlines and the contours of skin friction coefficient (C_f) obtained for the coarse grid resolution ($111 \times 101 \times 312$) are shown in Fig. 4 and Fig. 5 respectively. It is evident from these figures that the skin friction contours as well as the surface streamlines obtained by fixing transition are significantly different from the fully turbulent case before the transition location ($X/L = 0.2$) and beyond which they are identical. It was also observed that the azimuthal variation of the surface pressure coefficient for the fully turbulent and fixed transition is different upto the trip location and elsewhere they are identical (plots not shown here). The flow pattern (Fig. 4) clearly indicates that the present simulation could capture the primary and secondary separation as observed in the measurement data which confirms the adequacy of the grid resolution.

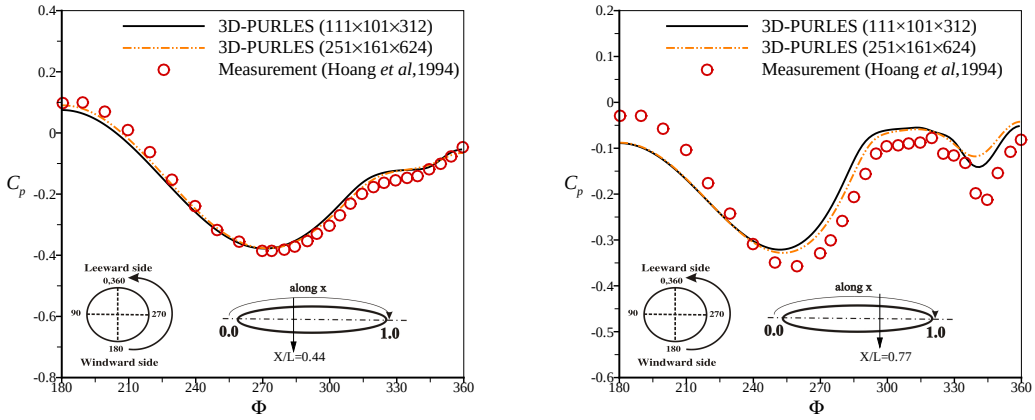

(a) Axial location $X/L = 0.44$ (b) Axial location $X/L = 0.77$

Figure 2: Effect of grid size on azimuthal variation of surface pressure coefficient using SST Model

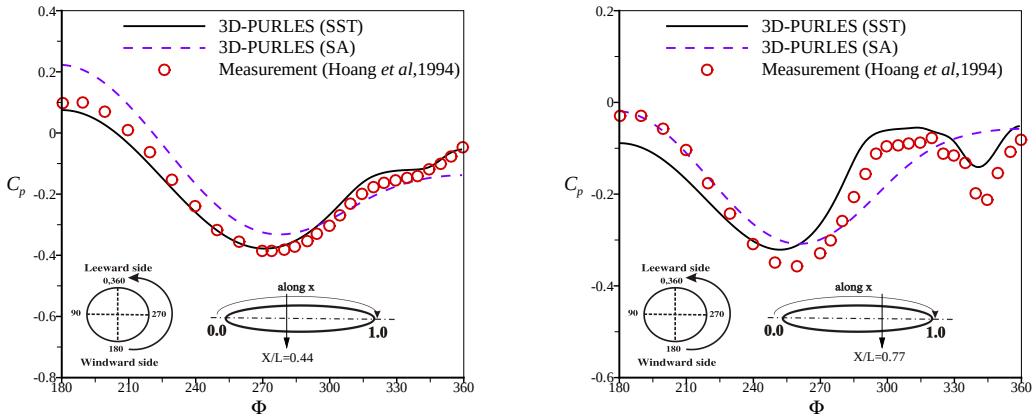

(a) Axial location $X/L = 0.44$ (b) Axial location $X/L = 0.77$

Figure 3: Effect of turbulence model on azimuthal variation of surface pressure coefficient using coarse grid

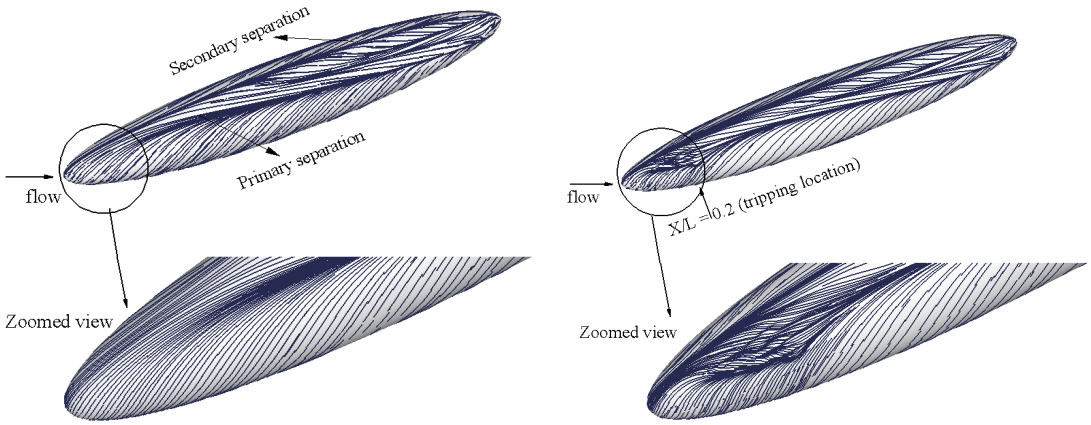

(a) Fully Turbulent (b) Fixed transition at $X/L = 0.2$

Figure 4: Surface streamlines on the prolate spheroid for coarse grid using SST Model

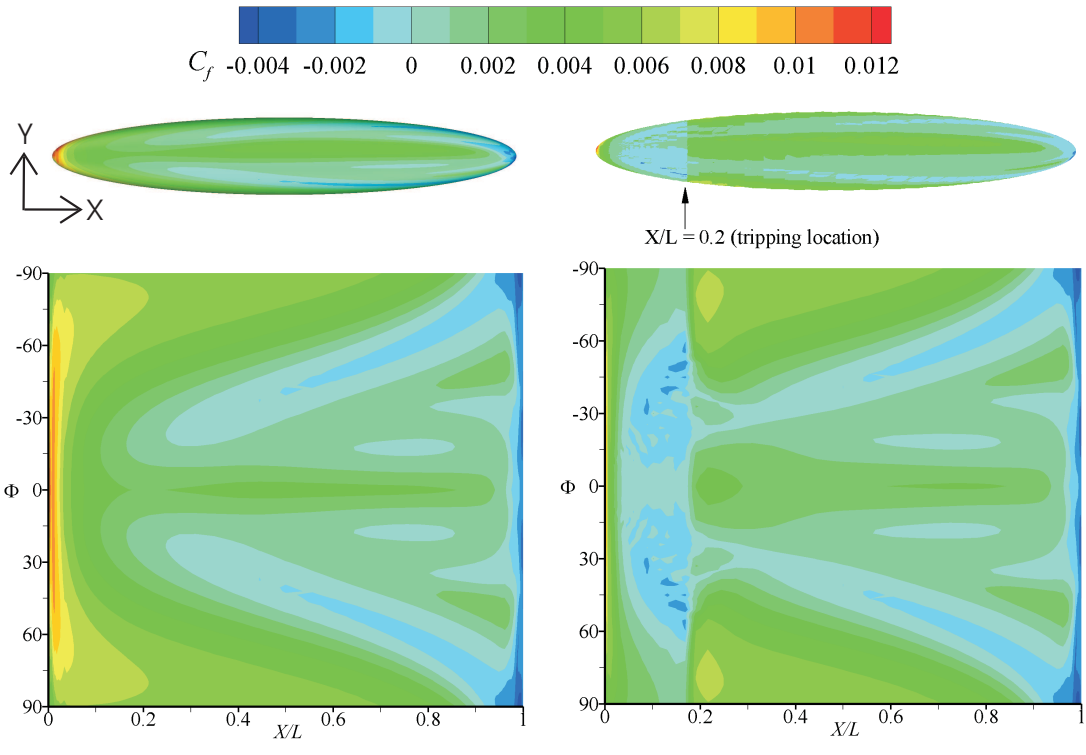

(a) Fully Turbulent (b) Fixed transition at $X/L = 0.2$

Figure 5: Contours of surface skin friction coefficient for coarse grid using SST Model

4 Concluding Remarks

The flow solution code 3D-PURLES has been successfully used to simulate fully turbulent and fixed transition case for flow around prolate spheroid at $\alpha = 20^{\circ}$ and $Re = 4.2 \times 10^6$. The azimuthal variation of the surface pressure coefficient at two axial locations in the fully turbulent region obtained using SST model are in reasonable agreement with the measurement. As part of the grid sensitivity study, doubling the grid size did not bring significant change in results. Encouraging results are obtained for the simulation carried out by fixing the transition onset location. Work is in progress to use transport equation based transition models to predict the onset and length of transition.

Acknowledgments

The authors wish to express their heartfelt thanks to the Head CTFD Division, CSIR-NAL, Bangalore for his support. We also deeply thank Director CSIR-NAL, Bangalore for his permission to publish this paper.

References

[1] K. M. Barber and R. L. Simpson. Mean Velocity and Turbulence Measurements of Flow around a $6:1$ Prolate Spheroid. *AIAA Paper 91-0255*, 1991.

[2] N. T. Hoang, T. G. Wetzel, and R. L. Simpson. Unsteady Measurements over a 6:1 Prolate Spheroid undergoing a Pitchup Maneuver. *American Institute of Aeronautics and Astronautics paper 1994-01979*, 35(6), 1994.

[3] P. K. Khosla and S. G. Rubin. A diagonally dominant second-order accurate implicit scheme. *Computers and Fluids*, 2:207–209, 1974.

[4] B. Rupesh Kotapati-Apparao, D. Kyle Squires, and R. James Forsythe. Prediction of a Prolate Spheroid Undergoing a Pitchup Maneuver. *American Institute of Aeronautics and Astronautics Paper 20030269*, 2003.

[5] S. Majumdar. Role of underrelaxation in momentum interpolation for calculation of flow with non-staggered grids. *Numerical Heat Transfer*, 13:125–132, 1988.

[6] F. R. Menter. Two-equation eddy-viscosity turbulence models for engineering application . *AIAA J*, 32:269–289, 1994.

[7] S. V. Patankar and D. B. Spalding. A calculation procedure for heat,mass and momentum transfer in three-dimensional parabolic flows. *International Journal of Heat and Mass Transfer*, 15:1787–1806, 1972.

[8] Pradeep Shetty, M.B.Subrahmanya, D.S. Kulkarni, and B.N.Rajani. CFD Simulation of flow past MAV wings. *Symposium on Applied Aerodynamics and Design of Aerospace Vehicle*, 2011.

[9] P. R. Spalart and S. R. Allamaras. A one-equation turbulence model for aerodynamic flow. *AIAA paper*, 92-0439, 1992.

[10] H. L. Stone. Iterative solution of implicit approximations of multidimensional partial differential equations. *SIAM Journal of Numerical Analysis*, 5:530–530, 1968.

[11] Meier. H. U., Michel. U., and Kreplin. H. P. The influence of wind tunnel turbulence on the boundary layer transition . *perspectives in turbulence studies, DFVLR, Gottingen, Germany*, pages 26–46, 1987.

[12] T. G. Wetzel, R. L. Simpson, and C. J. Chesnakas. Measurement of Three-Dimensional Crossflow Separation. *American Institute of Aeronautics and Astronautics Journal*, 36(4):557564, 1998.